

Contents lists available at ScienceDirect

Catena

journal homepage: www.elsevier.com/locate/catena





Mangrove expansion at poleward range limits in North and South America: Late-Holocene climate variability or anthropocene global warming?

Qiang Yao ^a, Marcelo Cohen ^{a,b,*}, Kam-biu Liu ^a, Daidu Fan ^c, Erika Rodrigues ^b, Kanchan Maiti ^a, Adriana Vivan de Souza ^b, Alejandro Antonio Aragón-Moreno ^d, Robert Rohli ^a, Dongxiao Yin ^a, Luiz Carlos Ruiz Pessenda ^e

- a Department of Oceanography and Coastal Sciences, College of the Coast and Environment, Louisiana State University, Baton Rouge, LA 70803, USA
- b Graduate Program of Geology and Geochemistry, Federal University of Pará, Rua Augusto Corrêa, 01 Guamá, CEP 66075-110 Belém, PA, Brazil
- ^c School of Ocean and Earth Science, Tongji University, 1239 Siping Road, Shanghai 200092, China
- d Tecnológico Nacional de México I. T. Chetumal, Av. Insurgentes 330, Chetumal, 77013 Quintana Roo, Mexico
- e CENA/14C Laboratory, University of São Paulo, Av. Centenário 303, Piracicaba CEP 13400-000, Brazil

ARTICLE INFO

Keywords: Ecotone Mangrove Palynology Poleward range limits Remote sensing Spatio-temporal analysis

ABSTRACT

Mangroves are expanding poleward in North and South America, but it is unclear whether such ecotonal-shift is an Industrial-Era phenomenon, or a recurring occurrence tied to Holocene climate variability. Our multi-proxy and remote sensing data from the U.S. Gulf Coast and southeastern Brazil suggest that the Industrial Era is the first time throughout the Holocene when mangroves were able to extend their distributions to the current boreal and austral range limits. A mangrove expansion of \sim 1.3 ha (from 0.002 to 1.33 ha), 103 ha (from 23 to 126 ha), and 1.42 ha (from 0.39 to 1.81 ha) are documented at Bolivar Flats (Texas, U.S.A.), Mississippi River Delta (Louisiana, U.S.A.), and Apalachicola (Florida, U.S.A.), respectively, since the early 2000s, suggesting that mangrove expansion in North America is a 21st -century phenomenon and likely governed by warming winters. In contrast, the relatively slow mangrove expansion (from 96.1 to 106 ha between 2003 and 2019) at the austral range limit is controlled primarily by available habitats with suitable salinity and sediment substrate.

1. Introduction

During the past few decades, mangrove encroachment into coastal marshes is documented across the tropical and subtropical regions in North and South America (Duke et al., 1998; Gilman et al., 2008; Osland et al., 2017; Ward et al., 2016), particularly near their boreal and austral limits in the two continents (Cavanaugh et al., 2014; Cohen et al., 2020a; Giri et al., 2011). In the conterminous U.S., the historical range limit of mangrove is located in Cedar Keys, Florida (Little & Viereck, 1971), with scattered populations along the Gulf of Mexico (GOM; Odum et al., 1982; Alongi, 2002; Osland et al., 2013; Fig. 1). In recent years, significant poleward mangrove migration has been observed along the coastlines of Texas (Comeaux et al., 2012), Louisiana (Michot et al., 2010), and Florida (Cavanaugh et al., 2014), as well as in Santa Catarina, Brazil - the mangrove austral limit (Cohen et al., 2020b). Although many previous studies have referred to these poleward mangrove migrations as part of the "tropicalization" of temperate ecosystems

(Saintilan et al., 2014; Osland et al., 2020), it is still unclear whether such encroachment is caused by the Industrial-Era climate change or tied to long-term global climate variability that expands and contracts the mangrove populations periodically (i.e., the Medieval Climate Anomaly and Little Ice age). However, most ecological studies can only record one episode of such "tropicalization" and very few paleoenvironmental reconstructions exist from the mangrove range limits in North (Rodrigues et al., 2021) and South America (Cohen et al., 2020b). Hence, large data gaps exist in the literature. Here, we extend the mangrove biogeography from decadal-scale to centennial- and millennial-scales by using time-tested methods - palynology, sedimentary and geochemical analyses, and radiometric dating on ten sediment cores to reveal the morphological and ecological transformation of four mangrove frontiers from North and South America - Bolivar Flats, Texas; Mississippi Delta, Louisiana; Apalachicola, Florida; and south Santa Catarina, Brazil (Fig. 1).

On the global scale, the environmental factors that govern the range

E-mail address: mcohen@ufpa.br (M. Cohen).

 $^{^{\}ast}$ Corresponding author.

and distribution of mangroves have been attributed to relative sea-level (RSL) rise, temperature (air and sea surface), precipitation, and human activities (Osland et al., 2016; Saintilan et al., 2020; Ward et al., 2016). On a regional scale, mangroves along the tropical Brazilian coast were more susceptible to fluvial discharge and sea-level fluctuation during the Holocene (Cohen et al., 2012, 2020a; Fontes et al., 2017; França et al., 2013, 2016), while their colonies at boreal and austral range limits are more sensitive to temperature change (Cohen et al., 2020b; Rodrigues et al., 2021). Previous studies have quantitatively linked empirical data of mangrove expansions with the aforementioned climatic and environmental observations (Cavanaugh et al., 2014, 2019; Snyder et al., 2021). However, some questions have yet to be answered. For example, is poleward mangrove migration synchronized and driven by the common influencing factors at the boreal and austral range limits? If so, is there a temporal threshold for such synchronized poleward mangrove migration? To investigate these paradoxes, we use high-resolution remote sensing data (obtained by drone and satellite) to track the mangrove expansion and contraction during the 21st century at the four study areas. We then compare the empirical data of mangrove dynamics with 32 years (1989-2020) of climatic and environmental observational records from the study regions to provide a synthetic view of the timeline and environmental factors controlling the mangrove dynamics at their poleward range limits in the light of climate changes. The overarching objective of this study is to reveal the potential timelines and causes for poleward mangrove migration from a paleoecological perspective.

2. Methods and materials

2.1. Study sites description

In the Neotropics, only four true mangrove species are found in the region: *Rhizophora mangle* (red mangrove), *Avicennia germinans* and *Avicennia schaueriana* (black mangroves), and *Laguncularia racemosa* (white mangrove). Along the poleward range limits, only dwarf (<2 m) black mangrove (A. germinans) is found in Texas and Louisiana, and red

and black mangroves have been observed in Apalachicola, FL, while black and white mangroves are found in south Santa Catarina (Alongi, 2002; Fig. 1). Bolivar Flats is a barrier island on the northeast Texas coast, about 80 km southeast of Houston. Field and drone survey shows that scrub black mangroves (<50 cm) are scattered among graminoids and succulent plants in saltmarshes \sim 100 to 500 m north of the beach barriers (Fig. S1).

Bay Champagne is a semi-circular backbarrier lagoon situated to the west of the current Mississippi Delta Lobe in coastal Louisiana (Fig. S2). The lagoon is surrounded by black mangroves and cordgrass (*Spartina alterniflora*). Shorelines near Bay Champagne are currently retreating at an alarming rate of ~12.5 m/yr due to subsidence, RSL rise, and hurricanes. A detailed description of the morphological setting of Bay champagne can be found in Liu et al. (2011) and Rodriguez et al. (2021).

Apalachicola National Estuarine Research Reserve marks the northernmost known present distribution of mangroves among the boreal study sites (Table S1). A small but dense black mangrove forest is established on Dog Island, and small colonies consisting of scattered individuals of scrub black mangroves (mostly < 50 cm) are present along St. George Island (Supplementary Fig. S3). Remarkably, some stands of red mangroves have been sighted on the barrier islands in recent years (Snyder et al., 2021). On the barrier islands, \sim 50–100 m of sandy beach occupies the Gulf shorelines. The backbarrier (2–10 m) marsh is occupied by shrubs (e.g., Ericaceae and *Myrica*), graminoids (Poaceae), and succulent plants (*Batis* and *Salicornia*), whereas pine savannas are found in the central areas of the island.

Santo Antonio lagoon, in Santa Catarina, Brazil, marks the present austral range limit for mangroves in South America. The lagoon has a salinity of 23‰, and the vegetation surrounding it consists primarily of Lentibulariaceae, Cyperaceae, and Poaceae families. Detailed description of mangroves in Santa Catarina can be found in Cohen et al. (2020b). Our field measurements show that salinities at Jaguaruna lagoon, Urussanga lagoon, and Arroio Lake are $\sim\!10,\ 1,\$ and $0\%,\$ respectively.

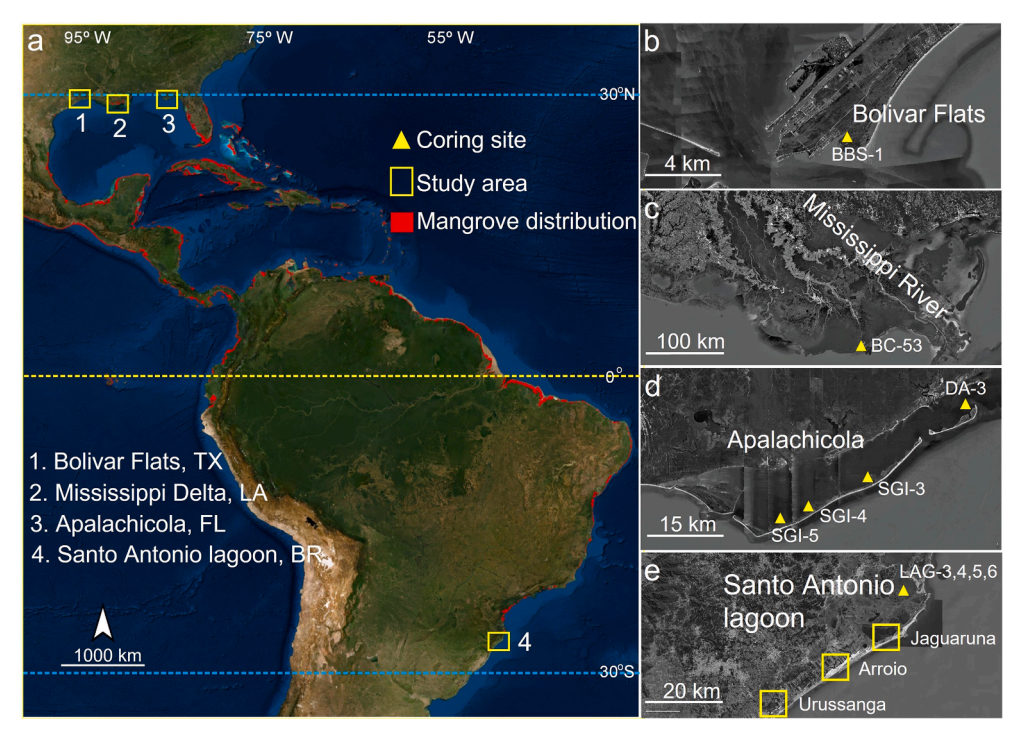


Fig. 1. Map showing the study areas and core locations. The red zones mark the mangrove distribution in North and South America (Spalding et al., 2010). The yellow triangles and squares mark the location of study areas and sediment cores. (For interpretation of the references to color in this figure legend, the reader is referred to the web version of this article.)

2.2. Fieldwork

Since 2014, continual fieldwork has been ongoing at four new mangrove frontiers with sustained mangrove population (according to extensive field survey and communication with local coastal managers) in North and South America - Bolivar Flats, Texas (Fig. 1b); Mississippi Delta, Louisiana (Fig. 1c); Apalachicola, Florida (Fig. 1d); and south Santa Catarina, Brazil (Fig. 1e). Ground vegetation surveys and approximately two dozen drone missions (~20 min and ~0.48 km² coverage per mission) were conducted at each study area during each field expedition. All cores were pushed in until refusal to capture the most complete depositional history possible. The description of cores from each study area is presented in the Supplementary Content (Table S1).

2.3. Spatio-temporal analysis of remotely sensing data

The high-resolution spatio-temporal analysis of remote sensing data used to document the decadal-scale mangrove dynamics was developed by Cohen et al. (2020b; Supplementary Fig S4). The spatial analysis used a combination of QuickBird satellite images (multispectral spatial resolution of 2.44 m/pixel) and images from Phantom 4 Advanced DJI drone equipped with GPS, inertial measurement, and digital 4 K/20MP (RGB) camera (spatial resolution of 1.6 cm/pixel at 60 m). All remote sensing images were processed and analyzed using Agisoft Metashape Professional version 1.6.2 and Global Mapper version 18. Drone images with a spatial resolution of 1.6 cm/pixel were then used as a reliable reference base to validate the classification developed on the QuickBird images. Field surveys and ground photos of fixed locations were also used to facilitate the identification of vegetation units on the QuickBird images. Each mangrove unit classified in the QuickBird image was visually checked and cross-validated to generate the highest accuracy possible. Details regarding image processing, vegetation identification, and data calibration are described in Supplementary Content.

2.4. Sedimentary and geochemical analyses

X-ray fluorescence (XRF) and Loss-on-ignition (LOI) analyses were performed for core BBS-1, BC-53, and DA-3 at a 1-cm interval to measure the elemental concentration (ppm) of major elements and the % wet weight for water and % dry weight for organics and carbonates throughout the core, following the standard laboratory procedure (Rodrigues et al., 2020). Grain-size analysis was performed at 1- to 5-cm intervals for cores BBS-1, BC-53, DA-3, and LAG-3,4,5,6 using a Beckman Coulter particle size analyzer (0.04–2000 μ m range.

2.5. Pollen analysis

Approximately 300 samples were taken from cores BBS-1, BC-53, DA-3, SGI-3,4,5, and LAG-3,4,5,6 for palynological analysis at 1–5 cm intervals to determine the percentages and concentrations of pollen, charcoal (>10 μm in size), foraminifera linings, and dinoflagellate tests. At least 300 grains of pollen and spores were counted for each sample to derive a statistical meaningful result, except for the intervals marked "pollen poor" (<50 grains per sample). One tablet containing $\sim\!20,583$ of *Lycopodium* spores was added to every sample as an exotic marker to aid the calculation of pollen concentration (grains/cm³). Details of standard pollen processing procedures and pollen concentration calculation can be found in Yao et al. (2015).

2.6. Chronology

Nineteen samples consisting of leaves, plant tissues, and treated bulk organic sediments (Yao et al., 2015) were sent to ICA Inc. in Florida and the University of Georgia-Center for Applied Isotope Studies for AMS ¹⁴C dating (Table S2). All radiocarbon dates were converted to calibrated

years before present (cal yr BP) using Calib 8.2 (https://calib.org) and rounded to the nearest decade. Nineteen samples from core DA-3 (0–38 cm) and 20 samples from core BC-53 (0–40 cm) were sent to the Marine Geochemistry Laboratory at Louisiana State University for ^{210}Pb and ^{137}Cs dating at 2 cm interval. Gamma-ray measurements were performed on a HPGe well type $\gamma\text{-ray}$ detector (GWL-120–15-LB-AWT, AMETEK). Excess $^{210}\text{Pb}\,(^{210}\text{Pb}_\text{ex})$ activity was determined by subtracting the supported $^{210}\text{Pb}\,(^{210}\text{Pb}_\text{su})$, equivalent to 226Ra) from total $^{210}\text{Pb}\,(^{210}\text{Pb}_\text{t})$. The surface sediment intervals (0–5 cm) were scanned in the detector for 48 hr. The excess ^{210}Pb data and sediment bulk density was used to calculate the sediment depositional history using the CRS (constant rate of supply) dating model with 2016 as the base year.

2.7. Environmental data collection and analysis

To determine the long-term trend of climatic and environmental variations at mangrove boreal and austral limits, 31 years (1990-2020) of daily observations of temperature and precipitation data at Bolivar Flats, Bay Champagne, Apalachicola, and Santo Antonio lagoon were received from U.S. Climate Data (https://www.usclimatedata.com/c limate/united-states/us) (USW00012923, USC00163433. USW00012832) and Brazil INMET (https://www.gov.br/agricultura/) (Urussanga#83923) meteorological stations. Sea-level (1990-2020) of the four study sites were retrieved from Galveston Pier 21 (#8771450), Grand Isle (#8761724), Apalachicola (#8728690), and La Paloma (#870-031) meteorological stations from NOAA CO-OPS (https://tidesandcurrents.noaa.gov/sltrends/).

Five time-series were calculated annually based on the daily dataset, which are winter accumulative freezing-degree-days (FDD - sum of daily degrees below 0 $^{\circ}$ C) (Table S3), winter (December through February in North America and June through August in South America) minimum air temperature (WMAT), winter average air temperature (WAAT), sea-level trend, and accumulated precipitation (AP).

To test which Parameter is more closely related to the expansion and contraction of mangroves, we calculated the accumulative change in mangrove areas (Δ mangrove area) between two remote sensing data points and correlate that with the accumulative changes in FDD (Δ FDD), WMAT (Δ WMAT), WAAT (Δ WAAT), sea-level (Δ SLC), and AP (Δ AP) between the same time intervals at each study site by using linear regression in the R package "IM Function" (Table S4).

3. Results

3.1. Multi-proxy paleoenvironmental dataset

Core BBS-1 (29°22′10.60″N, 94°44′0.20″W) consists of sand (90-45%), silt (25-10%), and clay (20-1%). Silty sand section (185-45 cm) can be divided into two zones (Fig. 2). Zone 1 (185-110 cm) is characterized by low pollen count and marked as "pollen poor". A radiocarbon date at 185 cm marks the bottom age of the core to be ~1890 cal yr BP. Above this barren section, the pollen of trees (*Pinus*, Quercus), herbs (Amaranthaceae, Asteraceae, Poaceae), and succulent plants (Salicornia) start to appear consistently in Zone 2 (110-45 cm), while non-pollen palynomorphs also increase. In particular, the salinity indicator - Cl/Br ratio (Liu et al., 2014; Yao et al., 2018, 2019) is consistently high in this silty sand section while the Ca/Ti ratio - an indicator for marine originated sediments (Yao et al., 2018) is relatively low (Fig. 2). Sediments gradually become finer upward, presenting a transition to sandy silt in Zone 3 (45–20 cm). This fining-upward trend is followed by an increase of organic and water content, while the Cl/Br ratio decreases by half and the Ca/Ti ratio becomes negligible. The pollen assemblage of Zone 3 resembles that of Zone 2 except for the disappearance of Solidago and Salicornia, whereas Poaceae, Amaranthaceae, and Asteraceae become more abundant, and marine microfossils, charcoal particles, and pollen concentration increase significantly. A significant increase of the Ca/Ti ratio, a decrease of non-

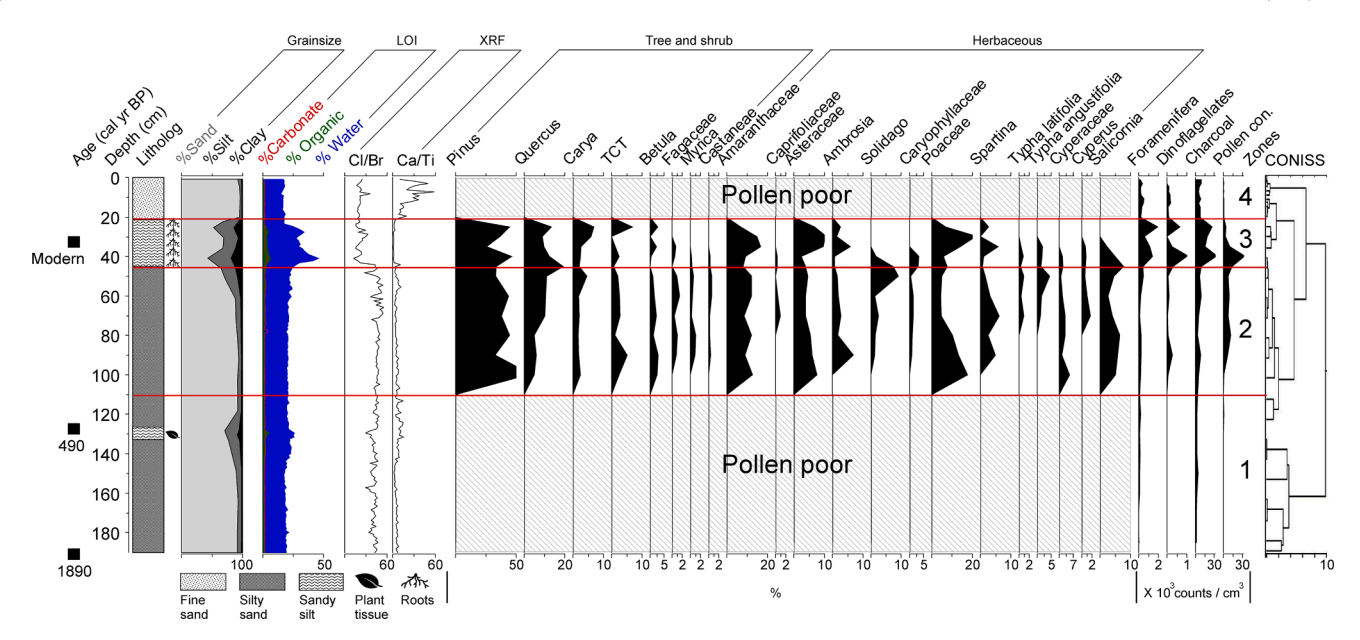


Fig. 2. Results of multi-proxy analyses of core BBS-1. The 185 cm-long core was taken from the Bolivar Flats, Texas, USA, in 2018 using a Vibra-corer (Table S1 and Fig. S1 in Supplementary Content). From left to right are the litholog, grainsize, LOI, and XRF diagrams of the core. The 2-σ calibrated age of accepted 14 C dates are listed at the left side of the figure at corresponding depths.

pollen palynomorphs, and the disappearance of pollen grains characterize the fine sand at the top 20 cm of core BBS-1 (Zone 4; Fig. 2). It is worth noting that no mangrove pollen was found throughout core BBS-1. In addition, radiocarbon dating revealed the age of two more sediment intervals at 32 cm (modern) and 127 cm (~490 cal yr BP; Table S2).

Core BC-53 ($29^{\circ}6'53.85''N$, $90^{\circ}10'57.87''W$) consists primarily of silty clay with a few coarse sediment layers embedded in the core. Zone 1 (222-140 cm) is characterized by a few centimeters of fine sand at the bottom and relatively high Cl/Br and Ca/Ti ratios, suggesting a marine influence since \sim 4760 cal yr BP (Fig. 3). Zone 2 (140-110 cm) is characterized by two coarse sediment layers (silt and sandy silt) and one high organic layer embedded in the silty clay. Zone 3 (110-45 cm) is

characterized by a decrease in both Cl/Br and Ca/Ti ratios (Fig. 3). The multi-proxy signature of Zone 2 strongly resembles the typical hurricane overwash layers found across the GOM – pollen poor, abundant marine microfossil (dinoflagellates), and alternating coarser sediments with a plant detritus layer on the top (Ryu et al., 2021; Yao et al., 2018). One radiocarbon date based on leaves found in the organic layer marks this paleo-hurricane strike at ~1610 cal yr BP. The pollen assemblages of Zones 1 and 3 are similar, with *Pinus*, Amaranthaceae, Poaceae, and *Typha* being the dominant pollen taxa. They strongly resemble those of the coastal marshes found in Louisiana (Yao et al., 2020), particularly at more inland areas northward of the mangrove swamps in Bay Champagne (Ryu et al., 2021). In Zone 4 (45–20 cm), *Batis maritima*, a succulent plant thriving in sandy saline environment, becomes the

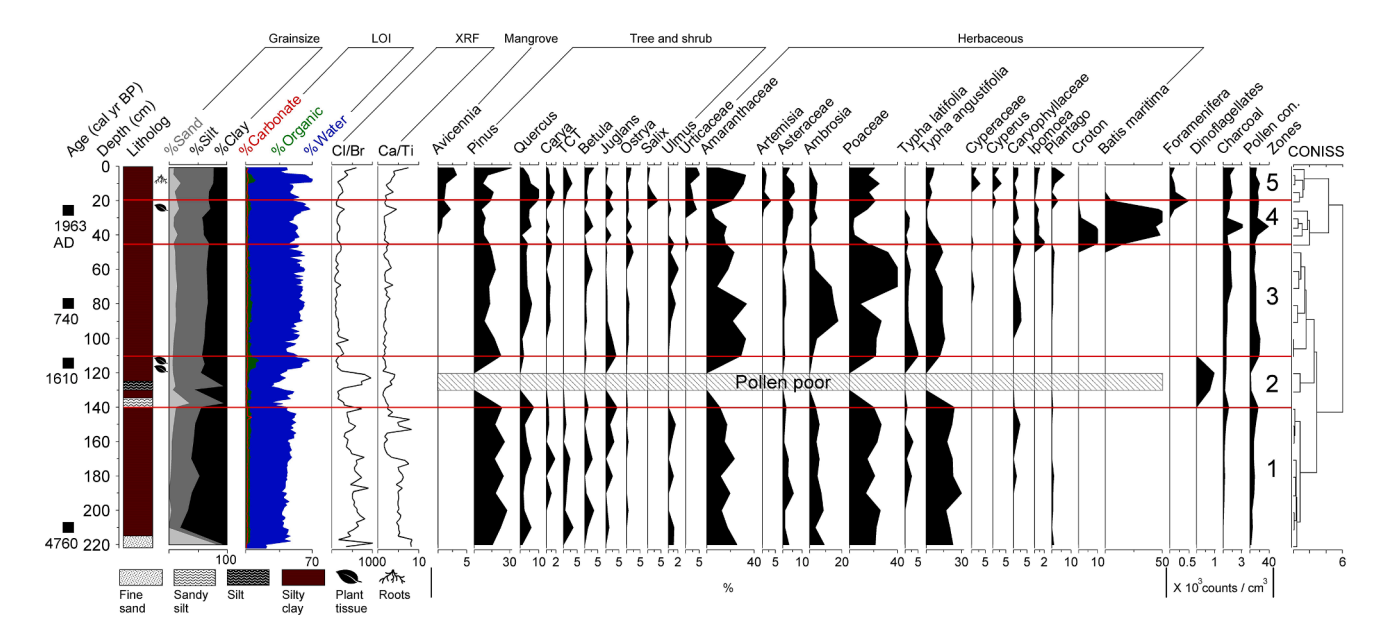


Fig. 3. Results of multi-proxy analyses of core BC-53. The 222 cm-long core was taken from a small pond surrounded by dense black mangrove (*Avicennia germinans*) shrubs on the landward edge of a backbarrier lake (Bay Champagne) near Port Fourchon in the Mississippi River Delta in Louisiana, USA, using a Russian peat borer (Table S1 and Fig. S2). From left to right are the litholog, grainsize, LOI, and XRF diagrams of the core. The 2- σ calibrated age of accepted 14 C dates is listed at the left side of the figure at corresponding depths.

dominant pollen type. *Avicennia* pollen starts to appear from the middle of this zone. Moreover, a ¹³⁷Cs peak is detected at 27 cm (Fig. S5a in Supplementary Content) and *Avicennia* pollen started to continuously appear from 35 cm. In Zone 5 (20–0 cm), black mangrove pollen, Cl/Br, Ca/Ti, and foraminifera consistently increase (Fig. 3), suggesting elevated marine influence at the site during the last several decades.

Four sediment cores (DA-3, SGI-3&4&5) were taken from Apalachicola, Florida (Table S1). In the main core DA-3 (29°49′33.74″N, 84°34'48.92"W), Zone 1 (38-22 cm) consists primarily of coarse sand characterized by high Cl/Br and Ca/Ti ratios (Fig. 4). This zone is characterized by very low pollen concentrations, mainly represented by arboreal pollen types (e.g., Pinus, Quercus, Amaranthaceae) and few marine microfossils. Above Zone 1, beach taxa (e.g., Amaranthaceae and Salicornia) and marine microfossils become dominant in Zone 2 (22-7 cm). Lithologically, a succession of upward fining (sandy silt) and then coarsening (silty sand) sediments with an increase of organic content and decrease of Cl/Br and Ca/Ti ratios characterizes this Zone. Zone 3 (7-0 cm) consists of silty sand and abundant fibrous roots and plant detritus with a thin layer of coarse sand at the core surface. Although black mangrove pollen consistently appears throughout the core, it becomes more abundant in Zone 3 (Fig. 4). A ¹³⁷Cs peak is detected at 11 cm and ²¹⁰Pb falls below the detection level from 20 cm downward (Fig. S5b&c). Based on the maximum nuclear fallout at 11 cm (CE 1963) and conventional ²¹⁰Pb conversion method (constant = 0.0311; Corbett & Walsh, 2015), vertical accretion rates obtained from ¹³⁷Cs and ²¹⁰Pb analyses are 0.19 cm/yr and 0.18 cm/yr, respectively, which are highly consistent. Under the assumption that the vertical accretion is also consistent, the core bottom likely dates back to the early 19th century. In addition, no mangrove pollen is found in cores (SGI-3, 4, 5) taken near three small mangrove colonies from St. George Island (Snyder et al., 2021) (Fig. S6). Among them, core SGI-3 dates back to \sim 1490 cal yr BP (Table S1).

At the austral range limit of mangroves in Brazil, four sediment cores (LAG-3,4,5,6) were taken from the tidal flats in Santo Antonio lagoon, southern Santa Catarina, using a Russian peat borer (Table S1). The multi-proxy record reveals that saltmarsh taxa (e.g., *Spartina* and *Acrostichum*) were the predominant pollen types throughout the sediment profiles in all four cores since ~1000 cal yr BP. After the mid-1950s, pollen of white (up to 20%) and black mangrove (up to 3%) started to appear in all 4 cores, and white mangrove subsequently became the dominant vegetation on the tidal flats in Santo Antonio lagoon (Fig. 5). Detailed descriptions of core LAG-3,4,5,6 proxy results can be seen Cohen et al., (2020b).

3.2. Spatio-temporal analysis of remote sensing data

Spatio-temporal analysis of satellite and drone data and field survey data show that mangroves have been expanding almost continuously at all four study areas since the early 21st century (Fig. 6). At Bolivar Flats (29°22′41.30″N – 29°21′53.19″N, 94°45′1.55″W – 94°43′29.31″ W; Fig. 6a), although individual black mangrove shrubs had been spotted periodically, approximately a dozen black mangroves have been sustained on the back-barrier low-lying areas since the early 2000s, according to oral communication with coastal managers from Bolivar Flats Shorebird Sanctuary. This small population proliferated after ~2010, when black mangroves started to invade coastal prairies previously dominated by herbs and succulent plants. In recent years (2013–2018), an expansion of over 1 ha of mangroves was recorded by satellite and drone images (Fig. 6a). Overall, the mangrove area expanded from 0.002 ha to 1.33 ha during the study period (2004–2018) and black mangrove is the only mangrove species recorded at this site.

At Bay Champagne, black mangrove is the sole recorded mangrove species during the study period, and an over four-fold increase in mangrove cover was recorded in our study area $(29^{\circ}09'-29^{\circ}\ 06'N, 90^{\circ}11'-90^{\circ}08'W; 900\ ha in size)$ since the early 21st century (Fig. 6b). In 2004, black mangroves (23 ha) primarily occupied the edge of the *Spartina* marsh fringing the water body. Since that time, continuous mangrove encroachment was observed in 2007 (44 ha) and 2012 (100 ha). A minor setback is observed in 2015 (90 ha) likely due to the hard winter freeze in the previous year, but the mangrove population recovered swiftly in 2017 (122 ha), and the encroachment resumed until 2019 (126 ha) despite another hard winter freeze in 2017 (Fig. 6b). Moreover, the maximum height of the studied mangrove population also increased from ~ 1 to ~ 2.3 m since the early 2000s (Cohen et al., 2021).

The progression of mangrove expansion in Dog Island, Apalachicola $(29^{\circ}50'7.97'' - 29^{\circ}48'21.31''N, 84^{\circ}35'22.01'' - 84^{\circ}34'3.80''W)$ is similar to that in Bolivar Flats (Fig. 6c). A continuous expansion with an over four-fold increase in mangrove cover is observed from 2006 (0.39 ha) to 2019 (1.81 ha). Although the mangrove colonies on the island consist primarily of black mangroves, several individuals of red mangrove (up to 1.5 m tall) were also found during the field survey (Fig. S3).

At Santo Antonio lagoon (28°28′23.25″ – 28°29′42.18″S, 48°52′6.27″ – 48°50′9.57″W), the earliest available remote sensing image reveals that dense patches (96.1 ha) of white mangroves already existed in the area in 2003 (Fig. 6d), and mangroves have been progressively invading tidal flats previously occupied by *Spartina* and *Acrostichum*. Since then, continuous mangrove encroachment is observed in 2009 (99.5 ha), 2012 (100.3 ha), 2013 (100.4 ha), 2016

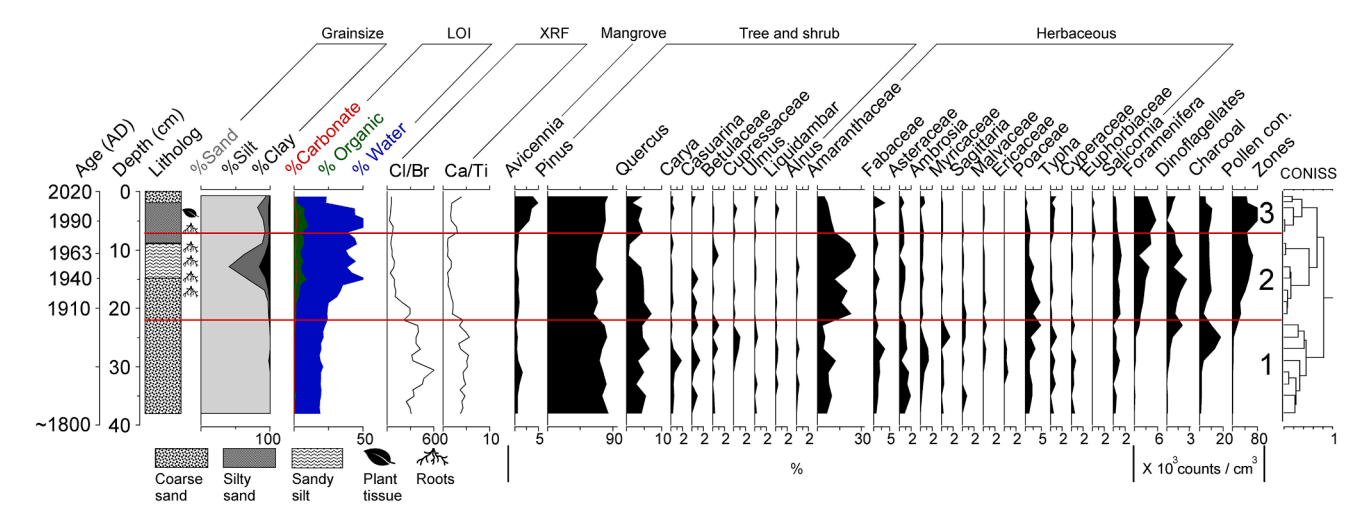


Fig. 4. Results of multi-proxy analyses of core DA-3. The 38 cm-long core was taken in a mangrove swamp on Dog Island, where the vegetation was dominated by *Avicennia germinans* with few *Rhizophora mangle* shrubs (Fig. S3b). From left to right are the litholog, grainsize, LOI, and XRF diagrams of the core. The 2-σ calibrated age of accepted ¹⁴C dates is listed at the left side of the figure at corresponding depths.

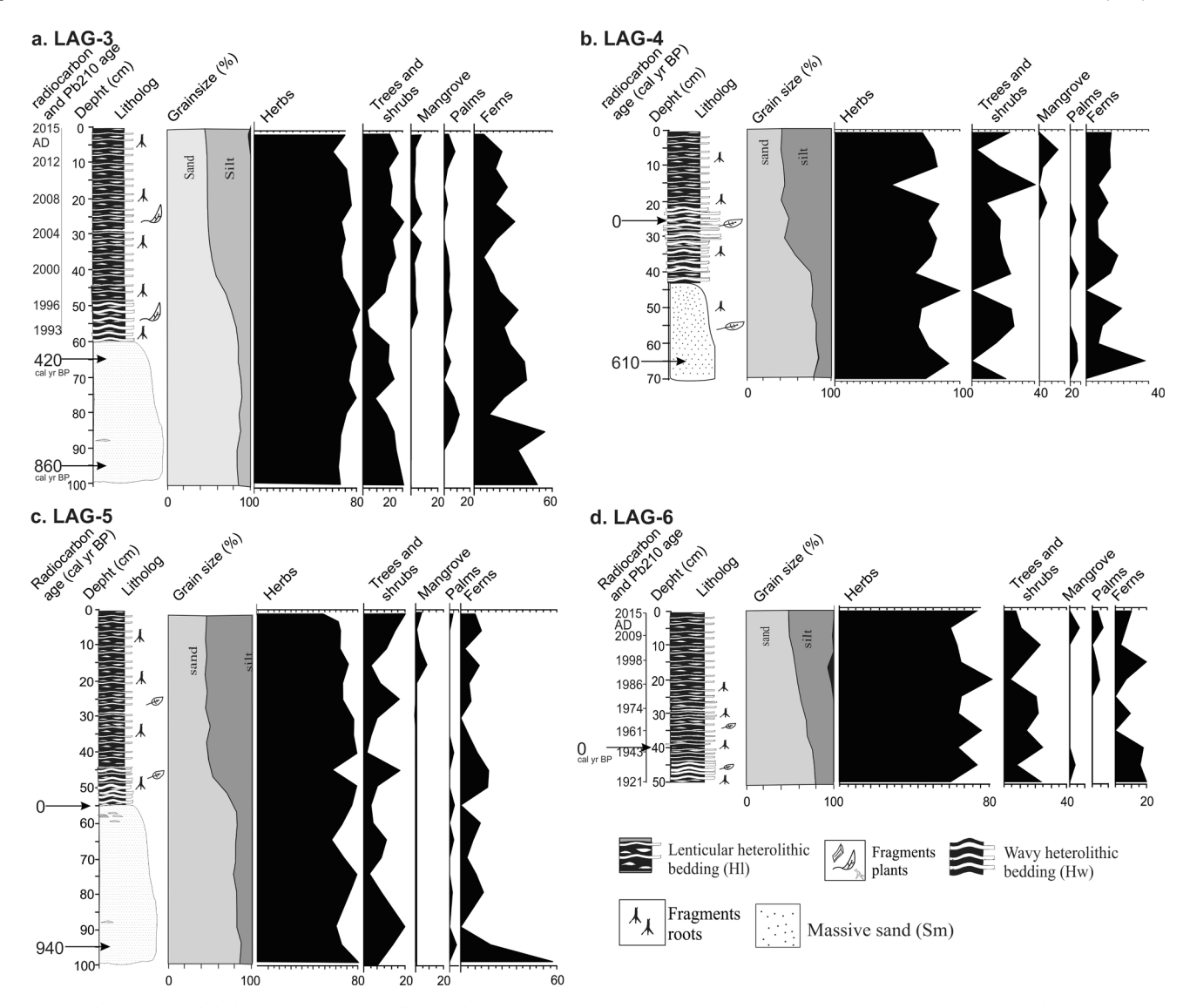


Fig. 5. From left to right is lithology, grainsize, and pollen results of core LAG-3 (a), LAG-4 (b), LAG-5 (c), and LAG-6 (d) from Santo Antonio lagoon, State of Santa Catarina, Brazil. These data are compiled and edited from Cohen et al. (2020b).

(102 ha), 2017 (104.3 ha), 2018 (105.5 ha), and 2019 (106.1 ha), an overall expansion of 6.6 ha from 2003 to 2019 (Fig. 6d; Cohen et al., 2020b).

3.3. Climatic and environmental variations associated with mangrove dynamics

From 1990 to 2020, meteorological stations near the four study areas across the Americas recorded an increasing trend in winter minimum air temperature (WMAT) and RSL (Fig. 7). The 31-year average annual WMAT and RSL rise at Bolivar Flats, Bay Champagne, Apalachicola, and south Santa Catarina are 10.64 °C, 8.03 °C, 9.89 °C, 10.84 °C, and 0.73 cm/yr, 0.82 cm/yr, 0.44 cm/yr, 0.33 cm/yr, respectively. In contrast, the observable trend in winter average air temperature (WAAT) and accumulated precipitation (AP) is more subtle at Bolivar Flats, Bay Champagne, Apalachicola, and Santo Antonio lagoon with a 31-year average annual WAAT and AP of 14.11 °C, 12.75 °C, 13.24 °C, 16.72 °C, and 1156 mm/yr, 1656 mm/yr, 1368 mm/yr, 1735 mm/yr (Fig. 7). In addition, the total accumulative winter FDD between 1989 and 2020 at Bolivar Flats, Bay Champagne, and Apalachicola are 91, 575.9, and 143 days (Table S3). No FDD was recorded near south Santa Catarina for the past 32 years (Table S3). A detailed breakdown of FDD

can be seen in Table S3 in the Supplementary Content.

At Bolivar Flats, a marginally significant negative correlation (R² = 0.8726, p-value = 0.066) is found between FDD and mangrove expansion (Fig. 8). Among other parameters, WMAT is found to be significantly correlated with mangrove expansion at Bay Champagne (R² = 0.754, p-value = 0.011) and Apalachicola ($R^2 = 0.925$, p-value = 0.038), while WAAT is significantly (marginally) correlated with mangrove expansion at Apalachicola ($R^2 = 0.99$, p-value = 0.062). No distinct association is found among mangrove expansion and any parameters at south Santa Catarina (Fig. 8). Overall, our quantitative analyses reveal that winter temperature is the key factor associated with mangrove expansion and contraction at the boreal limit study sites in North America. In contrast, mangrove area change is not associated with any of the five parameters at the austral limit sites between 1990 and 2020. A detailed breakdown of associations between the annual change in mangrove areas and Δ FDD, Δ WMAP, Δ WAAP, Δ SLC, and Δ AP can be seen in Table S4 in the Supplementary Content.

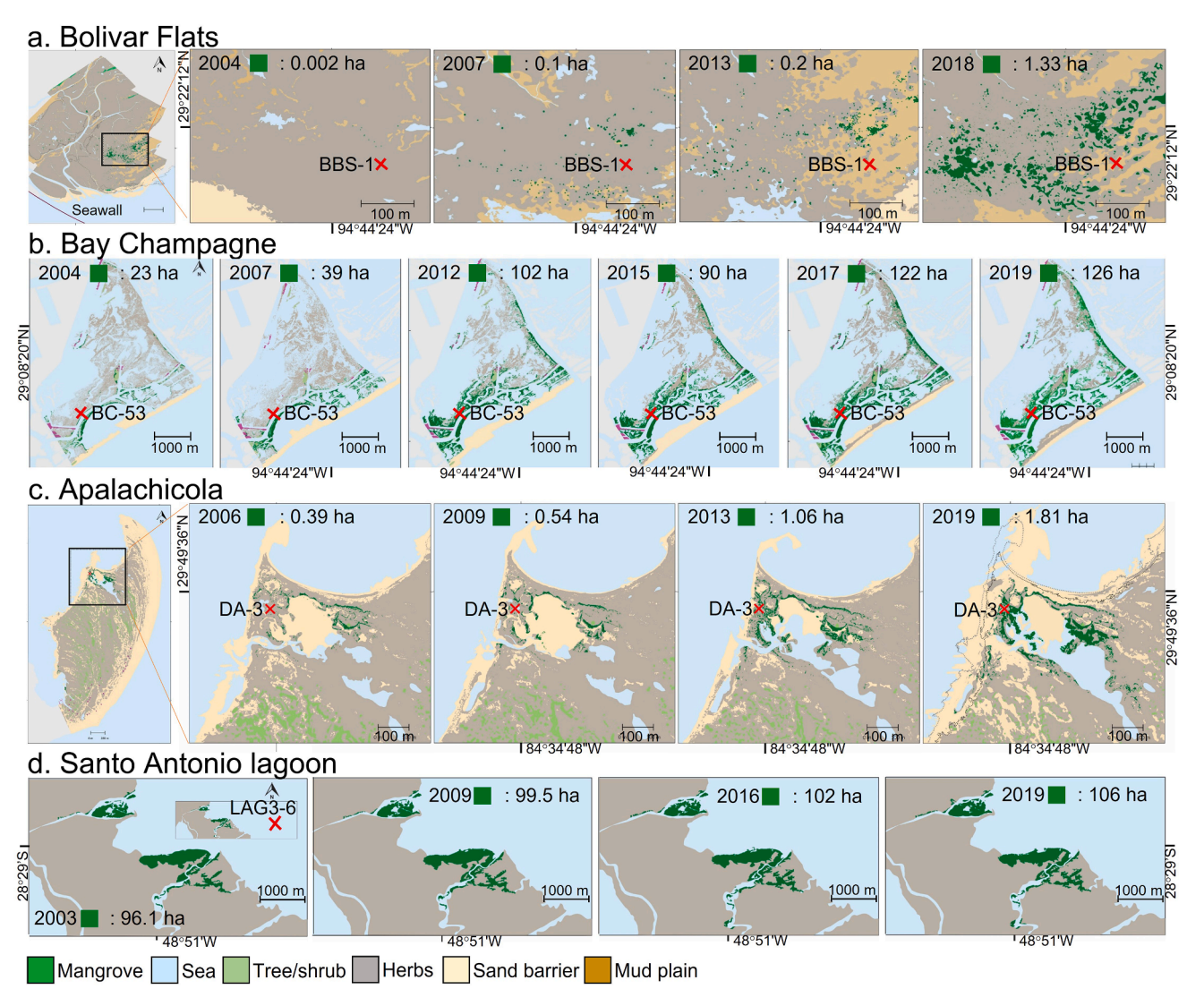


Fig. 6. Spatio-temporal analysis of mangrove areas. The dark green color marks mangroves at Bolivar Flats (a), Bay Champagne (b), Apalachicola (c), and Santo Antonio lagoon - Brazil (d), based on satellite and drone images between 2003 and 2019. The red crosses mark the coring locations, respectively. Each vegetation and landform type are color-coded for easy recognition. (For interpretation of the references to color in this figure legend, the reader is referred to the web version of this article.)

4. Discussion

4.1. The Holocene paleoenvironmental reconstruction from the mangrove range limits

The high-resolution multi-proxy and spatio-temporal analyses revealed the vegetation dynamics at mangrove poleward range limits in North and South America since the late Holocene. The substrate of cores BC-53, LAG-3, LAG-4, LAG-5, and LAG-6 are characterized by mud and sand with heterolithic beddings and abundant pollen grains, resembling a muddy tidal flat or a lagoon. The substrate of cores BBS-1 and DA-3 are comprised of fine sand and silt, resembling the modern tidal flats that mangroves are thriving upon. These sedimentary environments are all suitable for the establishment of mangroves (Woodroffe, 1982; Woodroffe and Grindrod, 1991).

At Bolivar Flats, the multi-proxy analyses show a decreasing trend in marine influence since \sim 1890 yr BP (Fig. 2). The bottom section of core BBS-1 (Zone 1) consists of mostly silty sand with very few pollens and non-pollen palynomorphs and characterized by high salinity (indicated by high Cl/Br ratio), suggesting a sandy environment under tidal influence. Above this barren section, although still in low concentration,

arboreal pollen types, herbs, and succulent plants start to appear in Zone 2 (Fig. 2). This pollen assemblage highly resembles the back-barrier coastal marsh that is found across the Texas coastlines today (Yao et al., 2019). Such morphological and vegetation transformation in Zone 2 suggest the formation of the barrier island, possibly due to sediment accretion facilitated by the longshore currents and the stabilization of sea-level during the Late-Holocene (Donoghue, 2011).

Moving to Zone 3, a sharp drop in the Cl/Br ratio indicates salinity decrease. The radiocarbon date at 32 cm in core BBS-1 marks the age of this stage to be in recent decades (Table S2). It is possible that the seawall to the west of Bolivar Flats accelerated the sediment accretion, decreasing the marine influence on the study site. This interpretation is supported by the remote sensing data, which shows a rapid progradation since the early 21st century (Supplementary Fig. S1). Accompanying this process is a significant increase in non-pollen palynomorphs and pollen concentrations and decrease in grainsize, indicating the flourishing of vegetation, which in turn traps more fine-grain sediments. This shift also marks the formation of the modern vegetation at the site today, a backbarrier saltmarsh dominated by graminoids and succulent plants with scattered scrub black mangroves (<50 cm) (Fig. S1). Interestingly, although field surveys, communications with Bolivar Flats Shorebird

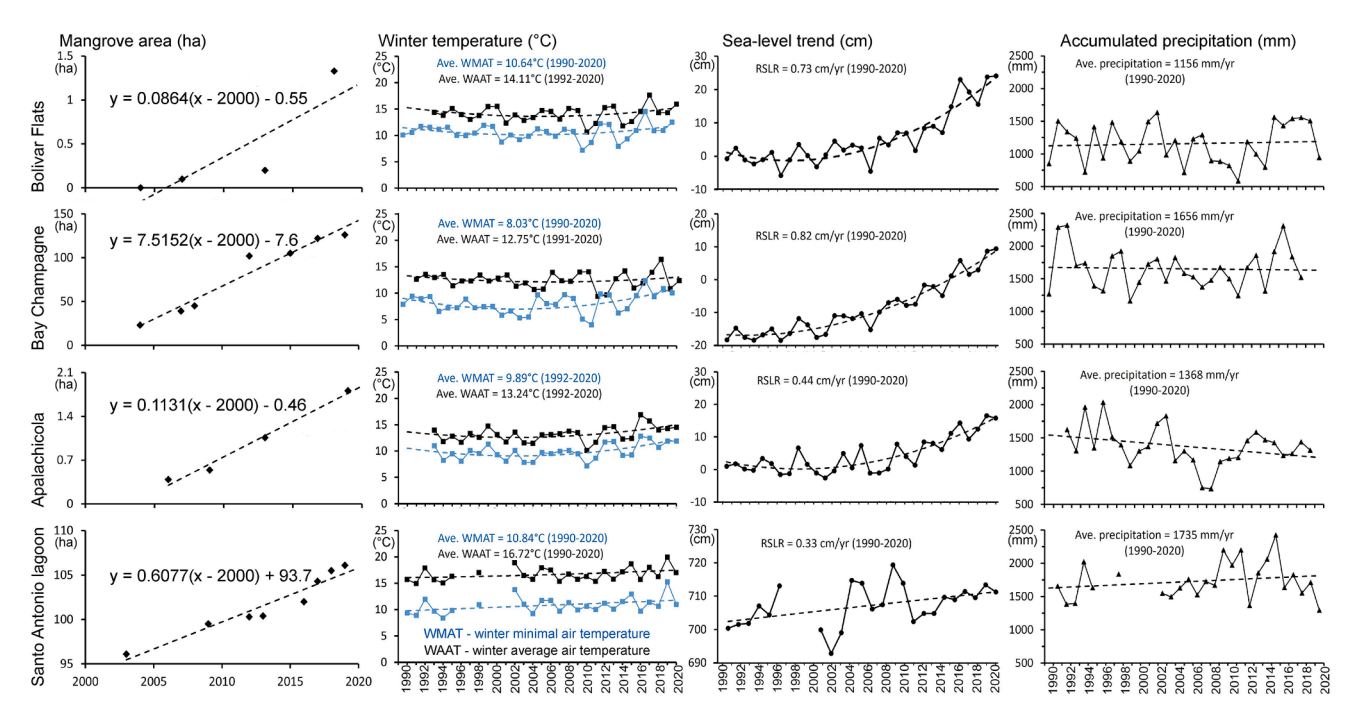


Fig. 7. Mangrove expansion and environmental parameters. The corresponding records of the four study sites are shown from the top to bottom. From left to right are the mangrove area changes since the early 2000s and the annual average of winter temperature (WMAT and WAAT), RSL, and accumulated precipitation trends during the 31-year study period (1990–2020) of the four study sites.

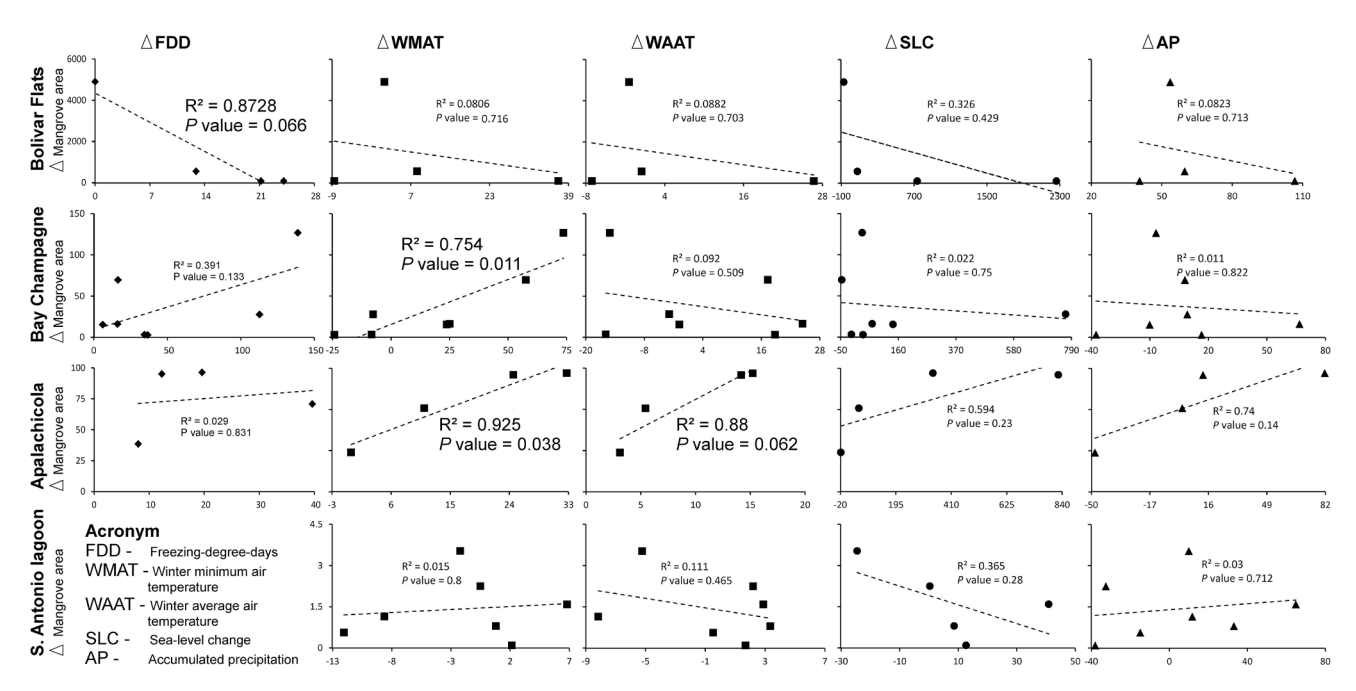


Fig. 8. Association between changes in mangrove area and climatic and environmental parameters. The corresponding record of the four study sites are shown from top to bottom. From left to right is the accumulative change in mangrove areas (Δ mangrove area) between two remote sensing data points plotted against the accumulative changes in FDD (Δ FDD), WMAT (Δ WMAT), WAAT (Δ WAAT), sea-level (Δ SLC), and AP (Δ AP) between the same time intervals at each study site by using linear regression. R^2 and p-value are shown on each plot and the statistically significant values are enlarged. No FDD is recorded in south Santa Catarina during the study period.

Sanctuary coastal managers, and remote sensing data all indicate the presence of black mangroves since the early 21st century (Fig. 6), no mangrove pollen were found throughout core BBS-1 (Fig. 2). We think the absence of mangrove pollen is due to the scarcity of the plants and their young age. The establishment of mangroves in Bolivar Flats is perhaps the latest, and the overall mangrove areas are also the smallest among all 4 study areas (Fig. 6a). Although black mangroves have been

observed for over a decade, their overall area was only 0.2 ha in 2013, hence, mature mangrove stands have only formed in Bolivar Flats in recent years (between 2013 and 2018). Considering a time lag of few years between flowering and accumulation of pollen rain in the surface soil is common in palynology (Havinga, 1967), it is reasonable to attribute this paradox to the recent establishment of black mangroves in Bolivar Flats. More importantly, it has been well-documented that

sediments accumulated in lagoons and tidal flats occupied by *Avicennia* or adjunct to *Avicennia* trees tend to have a good *Avicennia* pollen representation (Behling et al., 2001; Cohen et al., 2021b; Rodrigues et al., 2021). However, not a single *Avicennia* pollen was found in Zone 1&2 (Fig. 2), suggesting that *Avicennia* trees were absent at or near Bolivar Flats during the late Holocene.

At the Mississippi Delta, a more complex coastal morphodynamics and much longer mangrove history is revealed by the multi-proxy dataset (Fig. 3). The bottom sand layer in core BC-53 is characterized by high salinity (high Cl/Br ratio) and marine originated sediments (high Ca/Ti ratio), indicating a strong marine influence prior to ~4760 cal yr BP (Fig. 3). Overlying the sand layer was ~170 cm (Zones 1 & 3) of silty clay interrupted by a hurricane event layer (Zone 2). Previous studies documented that after the Mississippi Delta Lobe switched to further east positions (Day et al., 2007; McBride et al., 2007), excessive fluvial sediments were deposited near the current deltaic region that caused shoreline progradation since the Mid- to Late-Holocene (Yao et al., 2020). The grainsize and sedimentary signature of Zones 1 & 3 highly resemble those of the fluvial deposits originated from the Mississippi River (Rodrigues et al., 2021). Thus, the substrate of our study area was likely originated from Mississippi River since the Mid- to Late-Holocene

From 35 cm in core BC-53 (Zone 4), Avicennia pollen gradually started to appear. The ¹³⁷Cs peak at 27 cm marks the maximum nuclear fallout at CE 1963. Assuming a consistent sedimentation rate (0.704 mm/yr) between 27 (CE 1963) and 80 cm (740 cal yr BP), the first Avicennia pollen (35 cm) occurred at ~100 cal yr BP, marking the mangrove establishment in the Bay Champagne area between the late 19th to the early 20th century (Fig. 3). Moreover, Croton, Ipomoea, and especially Batis maritima become the dominant taxa in the pollen assemblage. These plants are adapted to saline and sandy environment and are commonly found in back-barrier marshes in Bay Champagne today, marking the formation of the modern coastal marsh in our study area (Rodrigues et al., 2021). Subsequently, the increase in black mangrove pollen and disappearance of Batis maritima in Zone 5 mark the formation of the modern mangrove swamp at Bay Champagne after the 1960s (Supplementary Fig. S2). Meanwhile, the increased in Cl/Br and Ca/Ti ratios in Zone 5 also indicates accelerated marine influence at Bay Champagne, in line with previous studies that a combination of natural and human processes, such as subsidence, coastal excavation, hurricanes, and sea level rise accelerated the coastal erosion at the current Mississippi Delta since the early 20th century (Lam et al., 2018; Schoolmaster et al., 2018). In sum, our multi-proxy dataset indicates that black mangroves started to appear in Bay Champagne since the late 19th to the early 20th century. Considering not a single mangrove pollen was found prior to 100 cal yr BP, and long distance transport (~200 km) of mangrove pollens by wind and current has been reported from the GOM (Yao et al., 2020), it is reasonable to conclude that no evidence of mangrove was found between the Mid-Holocene and the late 19th century in the vicinity of the Mississippi Delta (Rodrigues et al., 2021; Ryu et al., 2021).

At Apalachicola, our easternmost site along the northern Gulf Coast, the coastal morphological and ecological transformation is very similar to those recorded in Bolivar Flats. The multi-proxy record of core DA-3 suggests that the study area resembles a subtidal sandy environment during the19th century with little or no vegetation at the site (Zone 1). With the stabilization of the barrier island on the bay side, back-barrier marsh started to flourish at our coring site from the early 20th century (Zone 2). Since the 19th century, mangrove pollens have continuously appeared on Dog Island (Fig. 4). This result aligns with historical documents that recorded mangrove sightings as early as 200 years ago (Snyder et al., 2021). Nonetheless, only two or three mangrove pollen grains are found in each sample prior to the 1980s (Zone 3), suggesting a few individuals or a small population of mangroves. Since the 1980s, a significant surge of black mangrove pollen marks the establishment of the modern mangrove swamp on Dog Island, Apalachicola (Fig. 4). In

addition, not a single mangrove pollen is found in cores (SGI-3,4,5) taken from small mangrove patches on St. George Island (Supplementary Figs. S3), especially in core SGI-3 and SGI-4 that has a bottom age of ~1490 and 700 cal yr BP (Fig. S6), suggesting that mangroves on St. George Island have barely reached their flowering age or maturity. Thus, mature and sustained mangrove stands were formed on Dog Island after the 1980s and no evidence indicates mangrove establishment on Apalachicola and the vicinity prior to the 19th century.

At the austral mangrove range limits in Santo Antonio lagoon, south Santa Catarina, Brazil (Fig. 1e), our study area was a subtidal sandy environment occupied by saltmarshes from ~1000 cal yr BP to the recent centuries (Cohen et al., 2020b). Since the formation of the modern tidal flats in the 1950s, white and black mangroves started to gradually colonize the area and became the dominant species (Fig. 5). Nowadays, Santo Antonio lagoon receives sufficient marine influences with a salinity of 23 ‰, while the tidal flats are occupied by medium-sized white mangroves (≤5 m in height) and saltmarshes (e.g., *Spartina* and *Acrostichum*) with black mangroves growing sporadically in the vicinity (Cohen et al., 2020b; Soares et al., 2012).

Overall, except for the Mississippi River Delta where mature mangrove colonies have existed since the late 19th century (Fig. 3) (Rodrigues et al., 2021; Ryu et al., 2021), mature black and white mangrove stands have colonized their current boreal and austral range limits for only a few decades (Figs. 2-5). Moreover, no signs of mangroves were found at these study locations during the Medieval Climate Anomaly (~750-1000 cal yr BP), when the GOM was supposedly as warm as the present day (Richey et al., 2007). Thus, the above evidence suggests that the current poleward mangrove tropicalization is a post-Industrial-Era phenomenon instead of a recurring phenomenon tied to global climate variability, and the current range and magnitude of mangrove expansion has never been observed in the geological records since the Mid- to Late-Holocene. Considering the continuously rising temperature and sea-level trend in the Americas in the recent decades (Easterling et al., 2000; Medhaug et al., 2017), it is logical to suggest that the Industrial-Era is the first time during the Holocene when mangrove was able to expand their habitats poleward to ~29°N in North America (Bolivar Flats, Bay Champagne, and Apalachicola) and ~28°S in South America (Santo Antonio lagoon).

4.2. What drives mangrove expansion at boreal and austral limits?

At the mangrove boreal limit, the spatio-temporal analysis revealed significant mangrove expansion at all three sites along the northern GOM (Fig. 6). In particular, an over four-fold increase of \sim 1.3 ha, 103 ha, and 1.42 ha were record at Bolivar Flats (2004-2018), Bay Champagne (2004-2019), and Apalachicola (2006-2019), respectively, during the study period (Fig. 6). Although we are not disregarding the possibility that mangroves have already been expanding prior to the 21st century, our data indicate an undeniable outburst of mangrove proliferation after the 21st century at all boreal limit study sites. This evidence further suggests that poleward mangrove tropicalization is not just a post-Industrial-Era phenomenon, but more precisely a 21st century phenomenon, and such mangrove outburst is likely facilitated by the accelerated global warming in the 21st century (Fig. 7&8). The decadal climate record shows a clear rising trend of winter minimum temperature (WMAT) since 1990 CE (Fig. 7), whereas the change in WMAT is also significantly correlated with mangrove expansion at Bay Champagne and Apalachicola (Fig. 8). In Bolivar Flats, although no robust correlation is found between mangrove expansion and fluctuations in winter temperatures (Δ WMAT and Δ WAAT), we found that increase in mangrove area is (marginally) significantly correlated with the accumulative winter freezing-degree-days (FDD). Hence, winter temperature, especially winter freeze is still a primary factor that governs the mangrove dynamics at Bolivar Flats and other study sites along the Northern GOM.

Moreover, our dataset demonstrates that the relationship between

mangrove dynamics and climatic and environmental variability is likely more complicated than a singular threshold as described in previous studies. At Bay Champagne, where the largest mangrove colony (>126 ha) along the GOM is located, only WMAT is significantly correlated with mangrove coverage, although it had the highest FDDs (575.9) during the study period than any other boreal study sites (Table S3). In comparison, at Bolivar Flats, where the average WMAT (10.64 °C) and WAAT (14.11 °C) is the warmest and the total FDDs (91) is the lowest, only FDD is (marginally) significantly correlated with mangrove coverage (Fig. 8). Thus, we believe that over a multi-decadal timescale, among mangrove habitats where the winter climate is relatively warm, the occasional extreme winter freeze events are more detrimental to the survival and expansion of mangroves, especially if the populations are small and scattered. By contrast, after a dense mangrove forest has formed (i.e., Bay Champagne), mature mangroves can shelter the lowlying seedlings and propagules from freezing temperatures and attenuate the damage from freezing temperatures (Cohen et al., 2021; Osland et al., 2019), making the mangrove populations more resilient to winter freezes. Hence, the long-term fluctuations in the average WMAT assert more influence on the vitality of mangroves, even though Bay Champagne experienced more severe winters than any other study site over the past 31 years. As for Apalachicola, where FDD (143), WMAT (9.89 $^{\circ}$ C), and WAAT (13.24 $^{\circ}$ C) are mild, and a dense mangrove colony has formed in a small area (Figs. 5 & S4), while WMAT is still the most important factor limiting the expansion of mangroves, WAAT (R² = 0.88, p-value = 0.062) also plays a subtle role in controlling the overall mangrove population (Fig. 8).

In addition, our quantitative analyses have revealed no correlation between fluctuations in accumulated precipitation (AP) and mangrove coverage at Bolivar Flats, Bay Champagne, Apalachicola, and Santa Catarina, where the average annual AP (1990-2020) is 1156 mm, 1656 mm, 1368 mm, and 1735 mm, respectively (Fig. 7). This result aligns with the previous discovery of a precipitation threshold of 780 mm/yr, below which the mangrove vitality will be affected (Osland et al., 2016, 2017). The annual precipitation at all study areas is substantially above this threshold; hence, no correlation is observed. However, this observation implies that more abundant rainfall likely does not facilitate mangrove expansion either. Furthermore, a recent discovery indicates an upper RSL threshold of 0.61 cm/yr, beyond which the RSL rise will become detrimental to the survivability of mangrove populations (Saintilan et al., 2020). Interestingly, at Bolivar Flats and Bay Champagne, where the rate of RSL rise is 0.73 cm/yr and 0.82 cm/yr (1990–2020), much higher than the threshold (Fig. 7), no correlation was found between ΔSLC and mangrove coverage. For Bay Champagne, we believe this anomaly is related to the proximity of the study site to Mississippi River (Fig. 1). Studies from around the globe have discovered that the most extensive mangrove forests on the planet are associated with large river systems, which supplies plentiful sediments and nutrients to facilitate mangrove growth and compensate for environmental stressors, including rapid RSL rise (Thom et al., 1975; Walsh & Nittrouer, 2004; Yao and Liu, 2017). As for Bolivar Flats, although the tidal gauge data indicates an overall rising trend in the RSL (Fig. 7), our remote sensing data clearly show an accelerated sediment accretion at our study area from the early 21st century, likely facilitated by the seawall (see previous section in Discussion). However, more studies are needed to test these hypotheses and reveal the effects of Mississippi River and shoreline protection projects on the establishment of mangroves along the GOM.

At the Santo Antonio lagoon (Fig. 7a), no distinct correlation was observed in our quantitative analysis (Fig. 8), and all the climatic and environmental parameters are below the threshold that will impede the survival of mangroves (Fig. 7). What stops mangroves from expanding their colonies further poleward? We believe the answer lies in the unique coastal morphology and habitat availability along the southwestern Atlantic coastlines. Unlike the boreal range limit in North America, where the northern GOM (~28°N to 30°N) provides over 2000

km of coastlines for potential habitats for mangroves, the mangrove austral range limit (~28°S to 30°S) is comprised of only ~250 km of sandy coastal plains and lagoons with relatively low salinities (<10%; Fornari et al., 2012; Krauss et al., 2008 Fig. 1). More importantly, mangrove propagules require muddy or loamy substrate to anchor their roots (Gardel et al., 2011; Panapitukkul et al., 1998). However, coastal drift currents inhibit mud deposition and create sandy substrate along the southern Brazilian coastlines (Alves, 2009). Consequently, the majority of the coastlines at $\sim 28^{\circ} S$ to $30^{\circ} S$ in South Brazil is uncolonizable for mangrove, and the current mangrove austral range limit extends as far south as 28° 30S, inside a few lagoons in southern Santa Catarina (i. e., Santo Antonio lagoon), where the hydrodynamic conditions permit mud accumulation along their edges (Leite et al., 2021). Thus, mangrove expansion in South Brazil currently depends primarily on habitat availability and salinity and is not yet tied with other parameters discussed in previous sections.

During the fieldworks in South America, we also surveyed three potential mangrove habitats (Jaguaruna and Urussanga Lagoon and Arroio Lake) to the south of Santo Antonio lagoon (Fig. 1e) but did not find any mangroves (Fig. 9). Although their substrates are suitable for mangrove colonization, the salinities in these three areas are between 0 and 10‰, significantly lower than that in Santo Antonio lagoon (>20‰). It is likely that the low-salinity environment in these lagoons eliminates the competitive advantage (tolerance to high salinity) of mangroves over marsh species, resulting in a more hostile environment for mangroves to colonize. Remarkably, a relatively small mangrove expansion of 6.6 ha is still observed from 2003 to 2019 (Fig. 6) in Santo Antonio lagoon, suggesting that mangroves were thriving under a moderate rate of RSL rise (0.33 cm/yr) (Fig. 7) and expanding both landward and seaward (Cohen et al., 2020b).

5. Concluding remarks

This study documents the mangrove history from the Mid- to Late-Holocene at their poleward range limits in both North and South America and quantitatively links mangrove expansion with climatic and environmental variabilities at cross-continental scale using empirical data. Overall, our dataset indicates that poleward mangrove expansion is primarily driven by warming winters and a decrease in extreme winter freezes, in line with previous studies from North and South America (Cavanaugh et al., 2014, 2019; Cohen et al., 2020a&b; Osland et al., 2020; Soares et al., 2012). More specifically, along the Gulf of Mexico coast, where suitable substrates in the form of muddy tidal flats are abundant for mangrove establishment, low winter temperatures have played a more predominant role in limiting the poleward expansion of mangroves. By contrast, the migration of the austral mangrove range limit into more temperate zones, where winter is mild and RSL rise is much lower than the threshold (Saintilan et al., 2020), depends on the propagule transportation and marine influence into the lagoons. Under the projected continuous warming trend in the 21st century (IPCC, 2018), it is reasonable to assume that mangrove expansion will accelerate at their boreal range limits. In the case of southern Santa Catarina, a continuous sea-level rise should facilitate the marine incursion into Jaguaruna and Urussanga Lagoon and Arroio Lake and form a physiochemical condition in favor of mangrove establishment (Krauss et al., 2008).

We also acknowledge the limitations of this study. Although we retrieved data from the closest weather stations to our study areas, discrepancies might still exist between the observational data and the actual conditions at the mangrove sites. Moreover, as long as the winter temperature becomes mild enough, the presence or absence of mangroves near their latitudinal limitation may depend on an equilibrium involving the interplay among local factors such as biotic competition, human influence, stand density, and local hydrodynamic conditions related to tides, waves, and littoral currents, as well as sediment type and its rate of supply (Woodroffe and Grindrod, 1991;

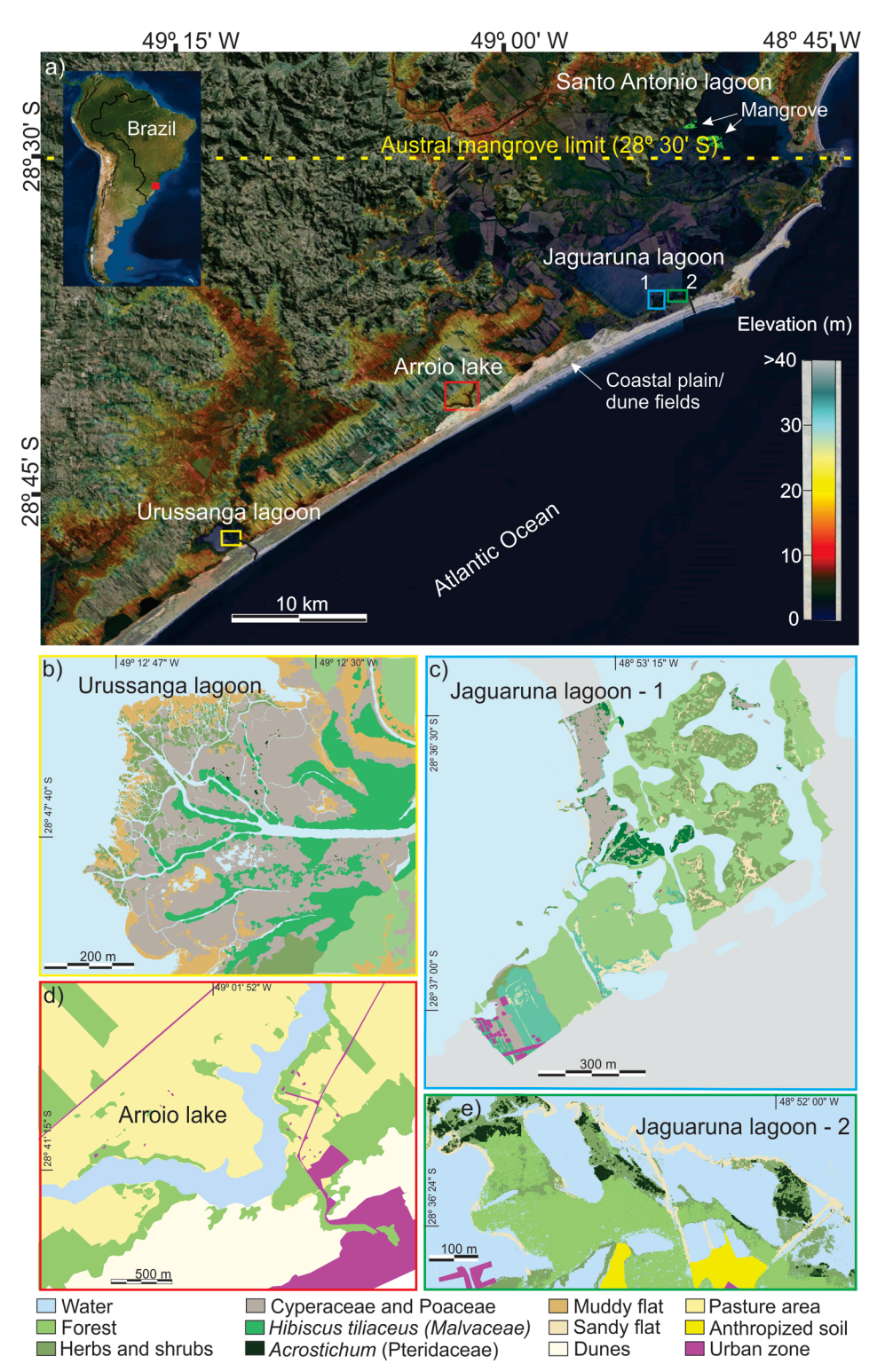


Fig. 9. Maps showing the terrain of the current austral mangrove range limit in South America. From the top to bottom: (a) south Santa Catarina, vegetation units at (b) Urussanga lagoon, (c) Jaguaruna lagoon 1, (d) Arroio Lake, and (e) Jaguaruna lagoon 2. Each vegetation and landform type are color coded for easy recognition.

López-Medellín et al., 2011; Montagna et al., 2011; Soares et al., 2012; Guo et al., 2013, 2017; Osland et al., 2020, Cohen et al., 2020). In particular, the proximity to a large river system (Bayou Lafourche) at Bay Champagne and the construction of a seawall at Bolivar Flats might have played a role in the recent history of mangrove establishment. Thus, more research is needed to reveal the long-term impacts of these local factors on poleward mangrove migration, and we hope this study provides a useful baseline for future studies.

Declaration of Competing Interest

The authors declare that they have no known competing financial interests or personal relationships that could have appeared to influence the work reported in this paper.

Data Availability

All datasets produced in this article will be stored at the Neotoma Paleoecology Database (https://www.neotomadb.org) upon publication and accessible to the public for free.

Acknowledgements

This study is funded by the U.S. National Science Foundation (BCS-1759715), Brazilian National Council of Scientific and Technological Development (CNPq 07497/2018-6, 403239/2021-4), the São Paulo Research Foundation (FAPESP 2020/13715-1), and State Key Laboratory of Marine Geology (MGK-1911). We thank Apalachicola National Estuarine Research Reserve and Bolivar Flats Shorebird Sanctuary for their logistical support before and during the field sample collection. We also thank Dr. Marlon França for his assistance.

Appendix A. Supplementary material

Supplementary data to this article can be found online at https://doi.org/10.1016/j.catena.2022.106413.

References

- Alongi, D.M., 2002. Present state and future of the world's mangrove forests. Environ. Conserv. 29 (3), 331–349. https://doi.org/10.1017/S0376892902000231.
- Alves, A.R., 2009. Long-term erosional hot spots in the southern Brazilian coast.

 J. Geophys. Res. Oceans 114 (C2), 2020. https://doi.org/10.1029/2008JC004933.
- Behling, H., Cohen, M.C.L., Lara, R.J., 2001. Studies on Holocene mangrove ecosystem dynamics of the Bragança Peninsula in north-eastern Pará, Brazil. Palaeogeogr. Palaeoclimatol. Palaeoecol. 167 (3-4), 225–242.
- Cavanaugh, K.C., Dangremond, E.M., Doughty, C.L., Williams, A.P., Parker, J.D., Hayes, M.A., Rodriguez, W., Feller, I.C., 2019. Climate-driven regime shifts in a mangrove-salt marsh ecotone over the past 250 years. Proc. Natl. Acad. Sci. USA 116 (43), 21602–21608. https://doi.org/10.1073/pnas.1902181116.
- Cavanaugh, K.C., Kellner, J.R., Forde, A.J., Gruner, D.S., Parker, J.D., Rodriguez, W., Feller, I.C., 2014. Poleward expansion of mangroves is a threshold response to decreased frequency of extreme cold events. Proc. Natl. Acad. Sci. U.S.A. 111 (2), 723–727. https://doi.org/10.1073/pnas.1315800111.
- Cohen, M.C.L., Camargo, P.M.P., Pessenda, L.C.R., Lorente, F.L., De Souza, A.V., Correa, J.A.M., Bendassolli, J., Dietz, M., 2021b. Effects of the middle Holocene high sea-level stand and climate on Amazonian mangroves. J. Quat. Sci. 36 (6), 1013–1027.
- Cohen, M.C.L., Figueiredo, B.L., Oliveira, N.N., Fontes, N.A., França, M.C., Pessenda, L.C. R., Souza, A.V., Macario, K., Giannini, P.C.F., Bendassolli, J.A., Lima, P., 2020a. Impacts of Holocene and modern sea-level changes on estuarine mangroves from northeastern Brazil. Earth Surf. Proc. Land. 45 (2), 375–392. https://doi.org/
- Cohen, M.C.L., Rodrigues, E., Rocha, D.O.S., Freitas, J., Fontes, N.A., Pessenda, L.C.R., de Souza, A.V., Gomes, V.L.P., França, M.C., Bonotto, D.M., Bendassolli, J.A., 2020b. Southward migration of the austral limit of mangroves in South America. CATENA 195, 104775. https://doi.org/10.1016/j.catena.2020.104775.
- Cohen, M.C.L., Pessenda, L.C.R., Behling, H., de Fátima Rossetti, D., França, M.C., Guimarães, J.T.F., Friaes, Y., Smith, C.B., 2012. Holocene palaeoenvironmental history of the Amazonian mangrove belt. Quat. Sci. Rev. 55, 50–58.
- Comeaux, R.S., Allison, M.A., Bianchi, T.S., 2012. Mangrove expansion in the Gulf of Mexico with climate change: Implications for wetland health and resistance to rising sea levels. Estuar. Coast. Shelf Sci. 96, 81–95. https://doi.org/10.1016/j.ecss.2011.10.003.
- Corbett, D. R., & Walsh, J. P. (2015). 210 Lead and 137 Cesium. In Handbook of Sea-Level Research. John Wiley & Sons, Ltd. https://doi.org/10.1002/9781118452547.ch24.
- Day, J.W., Boesch, D.F., Clairain, E.J., Kemp, G.P., Laska, S.B., Mitsch, W.J., Orth, K., Mashriqui, H., Reed, D.J., Shabman, L., Simenstad, C.A., Streever, B.J., Twilley, R.R., Watson, C.C., Wells, J.T., Whigham, D.F., 2007. Restoration of the Mississippi Delta: Lessons from Hurricanes Katrina and Rita. Science 315 (5819), 1679–1684.
- Donoghue, J.F., 2011. Sea level history of the northern Gulf of Mexico coast and sea level rise scenarios for the near future. Clim. Change 107 (1), 17–33. https://doi.org/10.1007/s10584-011-0077-x.
- Duke, N.C., Ball, M.C., Ellison, J.C., 1998. Factors influencing biodiversity and distributional gradients in mangroves. Global Ecology & Biogeography Letters 7 (1), 27–47
- Easterling, D.R., Karl, T.R., Gallo, K.P., Robinson, D.A., Trenberth, K.E., Dai, A., 2000. Observed climate variability and change of relevance to the biosphere. Journal of Geophysical Research: Atmospheres 105 (D15), 20101–20114. https://doi.org/10.1029/2000.ID900166.
- Fontes, N.A., Moraes, C.A., Cohen, M.C.L., Alves, I.C.C., França, M.C., Pessenda, L.C.R., Francisquini, M.I., Bendassolli, J.A., Macario, K., Mayle, F., 2017. The impacts of the middle Holocene high sea-level stand and climatic changes on mangroves of the Jucuruçu River, southern Bahia–northeastern Brazil. Radiocarbon 59 (1), 215–230.

Fornari, M., Giannini, P.C.F., Nascimento, D.R., 2012. Facies associations and controls on the evolution from a coastal bay to a lagoon system, Santa Catarina Coast, Brazil. Mar. Geol. 323-325, 56–68. https://doi.org/10.1016/j.margeo.2012.07.010.

- França, M.C., Cohen, M.C.L., Pessenda, L.C.R., Rossetti, D.F., Lorente, F.L., Buso Junior, A.Á., Guimarães, J.T.F., Friaes, Y., Macario, K., 2013. Mangrove vegetation changes on Holocene terraces of the Doce River, southeastern Brazil. Catena 110, 59–69.
- França, M.C., Alves, I.C.C., Cohen, M.CL., Rossetti, D.F., Pessenda, L.CR., Giannini, P.CF., Lorente, F.L., Buso Junior, A.Á., Bendassolli, J.A., Macario, K., 2016. Millennial to secular time-scale impacts of climate and sea-level changes on mangroves from the Doce River delta, Southeastern Brazil. The Holocene 26 (11), 1733–1749.
- Gardel, A., Gensac, E., Anthony, E., Lesourd, S., Loisel, H., Marin, D., 2011. Wave-formed mud bars: Their morphodynamics and role in opportunistic mangrove colonization. J. Coastal Res. 64, 384–387.
- Gilman, E.L., Ellison, J., Duke, N.C., Field, C., 2008. Threats to mangroves from climate change and adaptation options: a review. Aquat. Bot. 89 (2), 237–250. https://doi. org/10.1016/j.aquabot.2007.12.009.
- Giri, C., Ochieng, E., Tieszen, L.L., Zhu, Z., Singh, A., Loveland, T., Masek, J., Duke, N., 2011. Status and distribution of mangrove forests of the world using earth observation satellite data. Glob. Ecol. Biogeogr. 20 (1), 154–159. https://doi.org/ 10.1111/j.1466-8238.2010.00584.x.
- Guo, H., Zhang, Y., Lan, Z., Pennings, S.C., 2013. Biotic interactions mediate the expansion of black mangrove (A vicennia germinans) into salt marshes under climate change. Glob. Change Biol. 19 (9), 2765–2774.
- Guo, H., Weaver, C., Charles, S.P., Whitt, A., Dastidar, S., D'Odorico, P., Fuentes, J.D., Kominoski, J.S., Armitage, A.R., Pennings, S.C., 2017. Coastal regime shifts: rapid responses of coastal wetlands to changes in mangrove cover. Ecology 98 (3), 762–772.
- Havinga, A.J., 1967. Palynology and pollen preservation. Rev. Palaeobot. Palynol. 2 (1-4), 81–98. https://doi.org/10.1016/0034-6667(67)90138-8.
- Intergovernmental Panel on Climate Change. (2018). Global warming of 1.5° C. An IPCC Special Report on the impacts of global warming of 1.5° C above pre-industrial levels and related global greenhouse gas emission pathways, in the context of strengthening the global response to the threat of climate change, sustainable development, and efforts to eradicate poverty.
- Krauss, K.W., Lovelock, C.E., McKee, K.L., López-Hoffman, L., Ewe, S.M.L., Sousa, W.P., 2008. Environmental drivers in mangrove establishment and early development: a review. Aquatic Botany Aquat. Bot. 89 (2), 105–127. https://doi.org/10.1016/j. aquabot.2007.12.014.
- Lam, N., Xu, Y., Liu, K.-B., Dismukes, D., Reams, M., Pace, R., Qiang, Y.i., Narra, S., Li, K., Bianchette, T., Cai, H., Zou, L., Mihunov, V., 2018. Understanding the Mississippi River Delta as a coupled natural-human system: Research methods, challenges, and prospects. Water 10 (8), 1054. https://doi.org/10.3390/w10081054.
- Leite, R.A., Nóbrega, G.N., Leal, L.R.Z.C., Kiefer, M.C., Soares-Gomes, A., 2021. The colonization of a coastal lagoon by a mangrove ecosystem: Benefit or threat to the lagoon? Aquat. Bot. 171 (2021), 103362 https://doi.org/10.1016/J. AOUABOT.2021.103362.
- Little, E. L., & Viereck, L. A. (1971). Atlas of United States Trees: Florida, by E.L. Little, Jr (E. L. Little, Ed.). US Department of Agriculture, Forest Service.
- Liu, K.B., Li, C., Bianchette, T.A., McCloskey, T.A., Yao, Q., Weeks, E., 2011. Storm deposition in a coastal backbarrier lake in Louisiana caused by Hurricanes Gustav and Ike. J. Coastal Res. 1866–1870.
- Liu, K.-B., McCloskey, T. A., Ortego, S., & Maiti, K. (2014). Sedimentary signature of Hurricane Isaac in a *Taxodium* swamp on the western margin of Lake Pontchartrain, Louisiana, USA. *Proceedings of the International Association of Hydrological Sciences*, 367. https://doi.org/10.5194/piahs-367-421-2015.
- López-Medellín, X., Ezcurra, E., González-Abraham, C., Hak, J., Santiago, L.S., Sickman, J.O., 2011. Oceanographic anomalies and sea-level rise drive mangroves inland in the Pacific coast of Mexico. J. Veg. Sci. 22 (1), 143–151. https://doi.org/ 10.1111/j.1654-1103.2010.01232.x.
- McBride, R.A., Taylor, M.J., Byrnes, M.R., 2007. Coastal morphodynamics and Chenier-Plain evolution in southwestern Louisiana, USA: A geomorphic model. Geomorphology 88 (3-4), 367–422. https://doi.org/10.1016/j.geomorph.2006.11.013.
- Medhaug, I., Stolpe, M.B., Fischer, E.M., Knutti, R., 2017. Reconciling controversies about the 'global warming hiatus'. Nature 545 (7652), 41–47.
- Michot, T.C., Day, R.H., Wells, C.J., 2010. Increase in black mangrove abundance in coastal Louisiana. Louisiana Natural Resources News 4–5.
- Montagna, P. A., J. Brenner, J. Gibeaut, and S. Morehead. (2011). Coastal impacts. Pages 96–123 in J. Schmandt, G. R. North, and J. Clarkson, editors. The impact of global warming on Texas. Second edition. University of Texas Press, Austin, Texas, USA.
- Odum, W. E., McIvor, C. C., & Smith, T. J. (1982). The Ecology of the Mangroves of South Florida: A Community Profile. The Service.
- Osland, M.J., Day, R.H., Hall, C.T., Feher, L.C., Armitage, A.R., Cebrian, J., Dunton, K.H., Hughes, A.R., Kaplan, D.A., Langston, A.K., Macy, A., Weaver, C.A., Anderson, G.H., Cummins, K., Feller, I.C., Snyder, C.M., Friess, D., 2020. Temperature thresholds for black mangrove (Avicennia germinans) freeze damage, mortality and recovery in North America: Refining tipping points for range expansion in a warming climate. J. Ecol. 108 (2), 654–665. https://doi.org/10.1111/1365-2745.13285.
- Osland, M.J., Enwright, N., Day, R.H., Doyle, T.W., 2013. Winter climate change and coastal wetland foundation species: Salt marshes vs. mangrove forests in the southeastern United States. Glob. Change Biol. 19 (5), 1482–1494. https://doi.org/10.1111/gcb.12126.
- Osland, M.J., Enwright, N.M., Day, R.H., Gabler, C.A., Stagg, C.L., Grace, J.B., 2016. Beyond just sea-level rise: considering macroclimatic drivers within coastal wetland

- vulnerability assessments to climate change. Glob. Change Biol. 22 (1), 1–11. https://doi.org/10.1111/gcb.13084.
- Osland, M.J., Feher, L.C., Griffith, K.T., Cavanaugh, K.C., Enwright, N.M., Day, R.H., Stagg, C.L., Krauss, K.W., Howard, R.J., Grace, J.B., Rogers, K., 2017. Climatic controls on the global distribution, abundance, and species richness of mangrove forests. Ecol. Monogr. 87 (2), 341–359. https://doi.org/10.1002/ecm.1248.
- Osland, M.J., Hartmann, A.M., Day, R.H., Ross, M.S., Hall, C.T., Feher, L.C., Vervaeke, W. C., 2019. Microclimate influences mangrove freeze damage: Implications for range expansion in response to changing macroclimate. Estuaries Coasts 42 (4), 1084–1096. https://doi.org/10.1007/s12237-019-00533-1.
- Panapitukkul, N., Duarte, C.M., Thampanya, U., Kheowvongsri, P., Srichai, N., Geertz-Hansen, O., Terrados, J., Boromthanarath, S., 1998. Mangrove colonization: Mangrove progression over the growing Pak Phanang (SE Thailand) mud flat. ECSS 47 (1), 51–61. https://doi.org/10.1006/ECSS.1998.0343.
- Richey, J.N., Poore, R.Z., Flower, B.P., Quinn, T.M., 2007. 1400 yr multiproxy record of climate variability from the northern Gulf of Mexico. Geology 35 (5), 423. https:// doi.org/10.1130/G23507A.1.
- Rodrigues, E., Cohen, M.C.L., Liu, K.-B., Pessenda, L.C.R., Yao, Q., Ryu, J., Rossetti, D., de Souza, A., Dietz, M., 2021. The effect of global warming on the establishment of mangroves in coastal Louisiana during the Holocene. Geomorphology 381, 107648. https://doi.org/10.1016/j.geomorph.2021.107648.
- Ryu, J., Liu, K.-B., Bianchette, T.A., McCloskey, T., 2021. Identifying forcing agents of environmental change and ecological response on the Mississippi River Delta, Southeastern Louisiana. Sci. Total Environ. 794 (2021), 148730 https://doi.org/ 10.1016/j.scitotenv.2021.148730.
- Saintilan, N., Khan, N.S., Ashe, E., Kelleway, J.J., Rogers, K., Woodroffe, C.D., Horton, B. P., 2020. Thresholds of mangrove survival under rapid sea level rise. Science 368 (6495), 1118–1121.
- Saintilan, N., Wilson, N.C., Rogers, K., Rajkaran, A., Krauss, K.W., 2014. Mangrove expansion and salt marsh decline at mangrove poleward limits. Glob. Change Biol. 20 (1), 147–157. https://doi.org/10.1111/gcb.12341.
- Schoolmaster, D.R., Stagg, C.L., Sharp, L.A., McGinnis, T.E., Wood, B., Piazza, S.C., 2018.
 Vegetation cover, tidal amplitude and land area predict short-term marsh

- vulnerability in coastal Louisiana. Ecosystems 21 (7), 1335–1347. https://doi.org/10.1007/s10021-018-0223-7.
- Soares, M.L.G., Estrada, G.C.D., Fernandez, V., Tognella, M.M.P., 2012. Southern limit of the Western South Atlantic mangroves: Assessment of the potential effects of global warming from a biogeographical perspective. Estuar. Coast. Shelf Sci. 101, 44–53. https://doi.org/10.1016/j.ecss.2012.02.018.
- Spalding M, Kainuma M, Collins L (2010). World Atlas of Mangroves (version 3.1). A collaborative project of ITTO, ISME, FAO, UNEP-WCMC, UNESCO-MAB, UNU-INWEH and TNC. London (UK): Earthscan, London. 319 pp. URL: http://www. routledge.com/books/details/9781844076574, Data DOI: https://doi.org/ 10.34892/w2ew-m835.
- Thom, B.G., Wright, L.D., Coleman, J.M., 1975. Mangrove ecology and deltaic-estuarine geomorphology: Cambridge gulf-Ord river, Western Australia. The Journal of Ecology 63 (1), 203. https://doi.org/10.2307/2258851.
- Walsh, J.P., Nittrouer, C.A., 2004. Mangrove-bank sedimentation in a mesotidal environment with large sediment supply, Gulf of Papua. Mar. Geol. 208 (2-4), 225–248. https://doi.org/10.1016/j.margeo.2004.04.010.
- Ward, R.D., Friess, D.A., Day, R.H., Mackenzie, R.A., 2016. Impacts of climate change on mangrove ecosystems: a region by region overview. Ecosyst. Health Sustainability 2 (4), e01211. https://doi.org/10.1002/ehs2.1211.
- Woodroffe, C.D., 1982. Geomorphology and Development of Mangrove Swamps, Grand Cayman Island, West Indies. Bull. Mar. Sci. 32, 381–398.
- Woodroffe, C.D., Grindrod, J., 1991. Mangrove Biogeography: The Role of Quaternary Environmental and Sea-Level Change. J. Biogeogr. 18, 479–492. https://doi.org/10.2307/2845685
- Yao, Q., Liu, K.-B., Ryu, J., 2018. Multi-proxy characterization of Hurricanes Rita and Ike storm deposits in the Rockefeller Wildlife Refuge, southwestern Louisiana. J. Coastal Res. 85, 841–845. https://doi.org/10.2112/S185-169.1.
- Yao, Q., Liu, K.-B., Platt, W.J., Rivera-Monroy, V.H., 2015. Palynological reconstruction of environmental changes in coastal wetlands of the Florida Everglades since the mid-Holocene. Quaternary Research (United States) 83 (3), 449–458. https://doi. org/10.1016/j.yqres.2015.03.005.